UCRL--94686

DE86 011883

A VACUUM-TO-AIR INTERFACE FOR THE ADVANCED TEST ACCELERATOR BEAM DIRECTOR

G. E. Cruz
W. F. Edwards
D. P. Kavanagh
R. B. Addis
W. C. Weiss
C. W. Livenspargar

This paper was prepared for submittal to
1986 DARPA Conference
Albuquerque, NM
June 23-27, 1986

Lawrence Livermore National Laboratory

A VACUUM-TO-AIR INTERFACE FOR THE ADVANCED TEST ACCELERATOR BEAM DIRECTOR*

G.E.Cruz, W.F.Edwards, D.P.Kavanagh, R.B.Addis,
W.C.Weiss, and C.M.Livenspargar

Lawrence Livermore National Laboratory
University of California
Livermore, CA 94550

ABSTRACT

In this paper, we demonstrate the accomplishment of creating a vacuum-to-air transition to facilitate the Lawrence Livermore National laboratory's Advanced Test Accelerator (ATA) electron beam 1-Hz pulse rate. It is necessary that a pulsed particle beam go from a region at 10^{-6} torr through a 1-cm-diam maximum aperture into a region at 760 torr. This must be accomplished without the use of windows or solid barriers.

Two tests will be conducted on the vacuum-to-air interface. The first determines pressure profiles through 1.0-mm- and 10.0-mm-diam orifices. The second test employs an expendable foil and foil advancement mechanism. In this paper, we present the experimental results of the orifice test and compare the analytical results with the empirical results. The foil advancement test will be documented after the test is completed. The mechanism serves both as an orifice and as a fast-acting vacuum valve. In operation, the electron beam penetrates the thin foil, thereby creating an aperture of minimum geometry. During the balance of the pulse cycle, after the beam duration, the foil is advanced to seal the opening and recover the almost negligible loss in vacuum.

*Work performed jointly under the auspices of the U.S. Department of Energy by the Lawrence Livermore National Laboratory under contract W-7405-ENG-48 and for the Department of Defense under Defense Advanced Research Projects Agency ARPA Order No. 4395, monitored by Naval Surface Weapons Center under documents N60921-86-POW0001; and N60921-86-POW0002.

I. INTRODUCTION

The vacuum/air interface was designed to allow a viable vacuum-to-air transition for ATA that can also be used on other experiments on other machines. This interface has two components: a fast-action valve ($\leq$ 250 ms) that functions as a system shutter and a foil advancement mechanism that functions as a vacuum barrier. The hardware is an initial differential pumping design concept. The interface was designed to be compatible with the ATA machine; however, with a flange change it can be compatible with any machine. The fast valve and foil seal operate at a 1-Hz repetition rate; the pressure ranges from 1 torr to atmosphere. When the valve opens, the electron beam passes through the foil and the valve opening. When the beam pulse is complete, the valve closes and the foil advances 3 in. in readiness for the next pulse and the system is pumped to 1 torr. During operation, the vacuum system operates continually. It is necessary for the interface to be pumped back down to 1 torr within 1 s.

II. TEST PLAN

Bench testing is being performed to verify whether or not this design can operate in a 1-Hz mode. Figure 1 illustrates the first bench test setup. Testing will be done in two experiments, as follows:

EXPERIMENT 1 PURPOSES

1. To determine the system's pressure response over time as a result of:
   a. Pressurization through orifice diameters of 10 mm and 1 mm

b. Time exposed to atmospheric pressure

2. To determine the fast valve cycle times in response to:

   a. Varying the supply air pressure from 60 psi to 100 psi at 10-psi increments

   b. The pressure differential across the valve caused by the restricted orifice flows of objective 1.a.

EXPERIMENT 2 PURPOSES

1. To determine the system foil transfer characteristics:

   a. Under vacuum conditions vs atmospheric testing

   b. As a result of:

      (1) Orifice size

      (2) Time exposed to atmospheric pressure.

2. To determine the system pressure response over time as a result of:

   a. Pressurization through orifice sizes of 10 mm and 1 mm. The orifices are prepunched in the foil and spaced in alternating 3 in. lengths.

   b. Time exposed to atmospheric pressure.

3. To determine the fast valve cycle times in response to:

   a. Varying the supply air pressure from 60 psi to 100 psi at 10-psi increments

   b. The pressure differental across the valve caused by the restricted orifice flows of objective 2.a.

4. To establish and document system performance as compared to the findings of Experiment 1, orifice testing, and from this to provide system optimization

recommendations for mechanism upgrading.

Orifices of 1 mm and 10 mm were used in these tests because they represent two different electron beam diameters that cover the full beam diameter range.

III. ANALYTICAL RESULTS

Analytical results show that it takes 1.18 s to pump the 12.6-L vacuum/air interface volume down to 1 torr from atmosphere. These results are based on a valve cycle time of 0.55 s; for a cycle time of 0.25 s, the pump down time is 0.52 s. Because of the amount of gas load that has to be pumped from the interface, a separate ballast tank is required to maintain the interface vacuum requirements during repetitive cycles. The gas load that leaks through a 1-cm orifice during an operation cycle is 11,200 T-l/s, and the time the pressure differential is across the plate is 0.4 s. At the end of the operation cycle, the ballast tank pressure is 7.7 torr. It requires 1.7 s to pump down to 1.0 torr, 4.2 s to 0.1 torr, 9.2 s to 0.01 torr, and 21.3 s to 1 x 10^{-3} torr.

The net pumping speed of the ballast tank is 1404 L/s, which is not adequate for prolonged use of this system. Taking 21.3 s to pump the ballast to a 1 x 10^{-3} torr base pressure is too long to be effective for repetitive cycles. A larger amount of available net pumping speed is required for continuous operation on repetitive cycles because it does not take many cycles before the ballast is not able to keep up with the gas load. We expect that the fixed-orifice test can handle fewer repetitive cycles than the foil mechanism test because the foil mechanism has a much more conductance-limiting design. Because of space and cost considerations, the ballast tank we are using is small, but it is adequate to run our tests and prove the principle of the design.

IV. EMPIRICAL RESULTS

TEST RESULTS FOR THE 1.0-MM-DIAM ORIFICE

1. Single-Cycle Results

Pressure profile results exhibited in Figs. 2 through 6 show similarities that allow their results to be generalized.

Upon initialization of beamline valve cycling, note the immediate pressurization of the airside of the orifice to atmospheric pressure in less than 50 ms. This response indicates that the beamline valve is minimally effective unless it is cycled in less than 50 ms. Any cycle time greater than this allows the trapped volume to be completely pressurized to atmosphere. The trapped air is distributed throughout the system when the ballast valve is opened. Between 190 ms and 270 ms, the beamline valve closes. Note the slight depressurization shown in Fig. 3.

Data for the system pressure response on the vacuum side of the orifice, shown in Fig. 4, show that once the volume on the air side of the orifice is pressurized, the mass flowrate through the orifice becomes choked. Thus, the system pressurizes slowly until the trapped volume on the air side of the orifice is introduced to the system. As Fig. 4 shows, the 75-ms delay in pressure response from time zero (the beamline valve opening) is caused by a lack of instrument sensitivity. At time zero, the system is evacuated to the high 10^{-5} torr range, and it takes 75 ms to pressurize to the low-millitorr range, which is the low range of the instrument. The 100-ms delay between the time when the ballast valve opens and the time when the instruments register the pressure increase from the trapped air volume is a function of the ballast tank volume.

Referring to Fig. 7 for the vacuum side of the orifice, note that the system stabilizes at 2.65 torr between 500 ms and 600 ms from the beamline valve opening. The final pressure seems to be primarily a function of the entrapped volume of air on the air side of the orifice, only secondarily a function of orifice diameter.

2. Multicycle Results

The multicycle results shown in Figs. 5 and 6 demonstrate that the system pressure response is dependent upon the entrapped air volume on the air side of the orifice, after beamline cycling. Figure 6 shows that constant pressure increases at the system stabilization points during multicycling. These points are nearly linear, except for the point at which pump efficiency increases as pressure increases, which accounts for the slight nonlinearity.

Pressure response is constant for each cycling, and extrapolation of the system response to any number of cycles can be made up to the time of system saturation.

TEST RESULTS FOR THE 10.0-MM-DIAM ORIFICE

1. Single cycle results

Figure 8 is similar to the corresponding responses in Fig. 3. In contrast to the 1.0-mm orifice, the vacuum side of the 10.0-mm orifice experiences an immediate pressurization response that lasts for 150 ms. The mass flow rate becomes choked at 8 torr, as shown in Fig. 9. After 150 ms and during the beamline valve closing sequence, the vacuum side of the orifice experiences a parallel depressurization. System stabilization is attained upon opening the ballast valve. At the time of system stabilization, note that the 10-mm orifice accounts for approximately a 1.25-torr difference in stabilization pressures as compared with the 1.0-mm orifice.

As shown in Fig. 3 for the 1.0-mm orifice, the system seems to be dependent primarily on the entrapped air volume on the air side of the orifice.

2. Multicycle Results

Figures 10 and 11 are similar to the 1.0-mm orifice results shown in Figs. 5 and 6, thus confirming similar conclusions and responses.

Figure 10 illustrates the consistent system response on the air side of the orifice, whereas Fig. 11 illustrates the system stabilization pressure linear response caused by the constant air volume absorption by the tank after each cycle. Again, the slight nonlinearity is caused by greater pump efficiency at higher pressures. System pressure responses can be extrapolated up to the system saturation value of 375 torr.

V. SUMMARY

The first of our two tests showed a need for system design modifications. Based on the test results, two major design considerations need to be addressed: reduction of the entrapped air volume on the air side of the orifice and an increase in the ballast system pumping capacity. Results also indicate that minimizing the orifice diameter and increasing the beamline valve operation speed would help optimize system operation.

Empirical results for the second experiment are not available at this time because the tests are in progress; however, they will be published as an addendum to this paper when they are available. Figures 12 through 15 illustrate the foil advance mechanism used in Experiment 2.

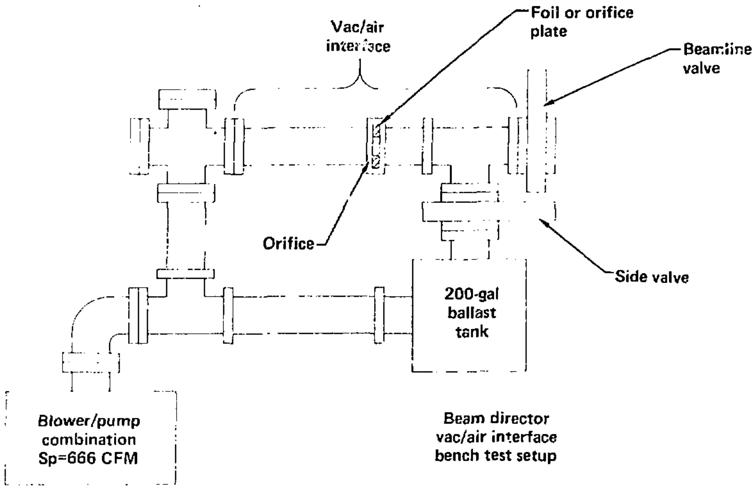

Fig. 1 Beam director vacuum/air interface bench test setup.

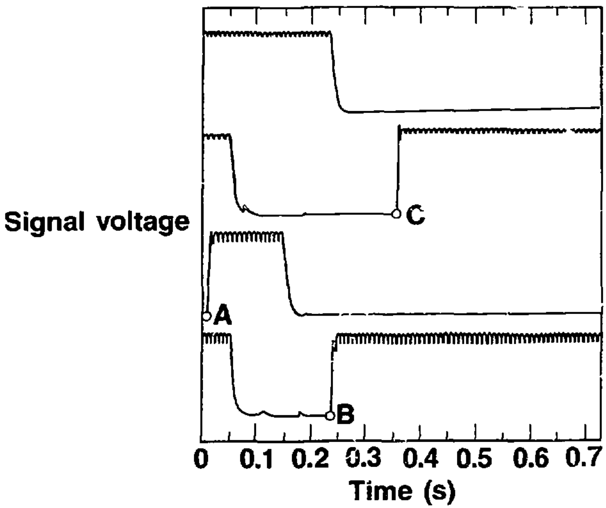

A. Beamline valve open command, 0.000 s
B. Beamline valve close confirmed, 0.223 s
C. Ballast system valve open confirmed, 0.343 s

Fig. 2 Valve timing response. Single pulse.

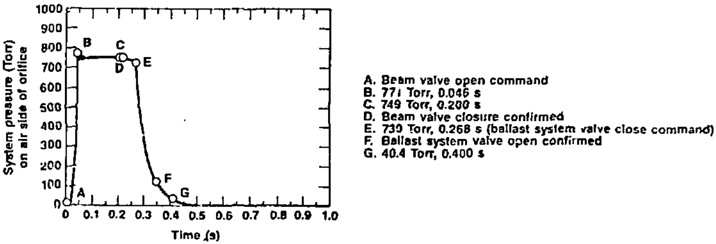

Fig. 3 Averaged results of system pressure response on air side of 1.0-mm ϕ orifice. 80-psi valve actuator pressure. Single cycle.

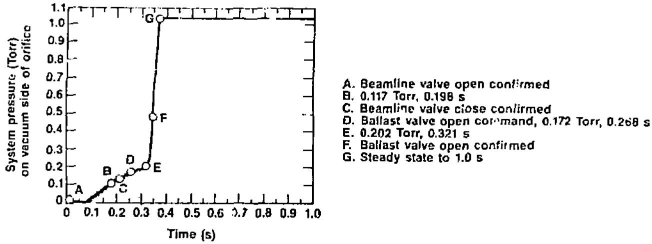

Fig. 4 Averaged results of system pressure response on vacuum side of 1.0-mm ϕ orifice. 80-psi valve actuator pressure. Single cycle.

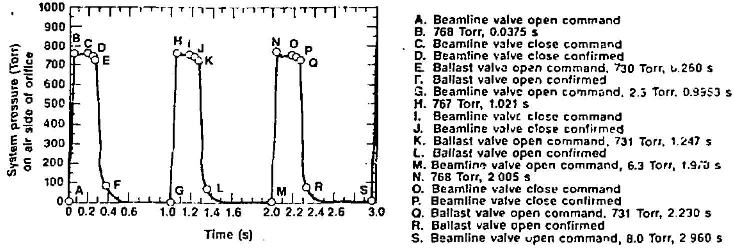

Fig. 5 Averaged results of system pressure response on air side of 1.0-mm φ orifice. 80-psi valve actuator pressure. Multiple cycles.

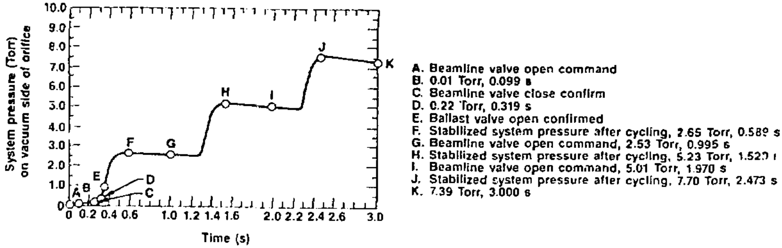

Fig. 6 Averaged results of system pressure response on vacuum side of 1.0-mm φ orifice. 80-psi valve actuator pressure. Multiple cycles.

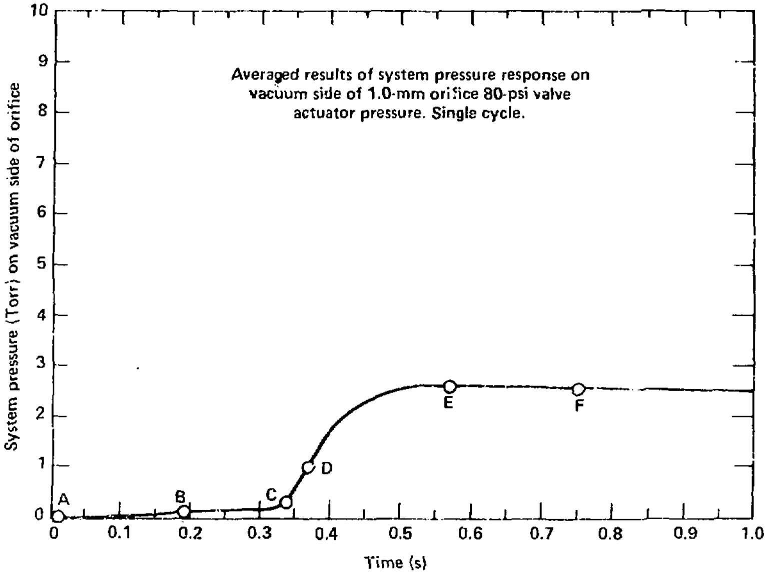

A. Beamline valve open command
B. Beamline valve close confirmed
C. Ballast valve open confirmed
D. 1.05 Torr, 0.372 s
E. Highest system pressure after cycling, 2.65 Torr, 0.570 s
F. 2.60 Torr, 0.750 s

Fig. 7 Averaged results of ballast system pressure response on air side of 1.0-mm ϕ orifice. 80-psi valve actuator pressure. Single cycle.

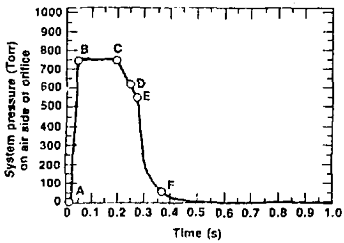

A. Beamline valve open command
B. 762-Torr, 0.048 s
C. Beamline valve close command, 746 Torr, 0.188 s
D. Beamline valve close confirmed, 590 Torr, 0.250 s
E. Ballast valve open command, 543 Torr, 0.271 s
F. Ballast valve open confirmed, 50 Torr, 0.370 s

Fig. 8 Averaged results of system pressure response on air side of 10.0-mm φ orifice. 80-psi valve actuator pressure. Single cycle.

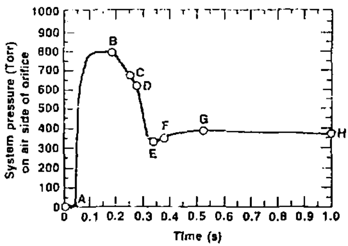

A. Beamline valve open command
B. Beamline valve close command, 7.97 Torr, 0.190 s
C. Beamline valve close confirmed, 6.70 Torr, 0.250 s
D. Ballast valve open command, 6.12 Torr, 0.276 s
E. 3.25 Torr, 0.346 s
F. Ballast valve open confirmed
G. Highest system pressure after cycling, 3.93 Torr, 0.524 s
H. 3.73 Torr, 1.00 s

Fig. 9 Averaged results of system pressure response on vacuum side of 10.0-mm φ orifice. 80-psi valve actuator pressure. Single cycle.

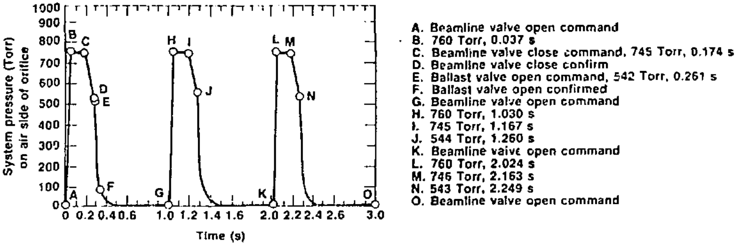

Fig. 10 Averaged results of system pressure response on air side of 10.0 mm ø orifice. 80-psi valve actuator pressure. Multiple cycles.

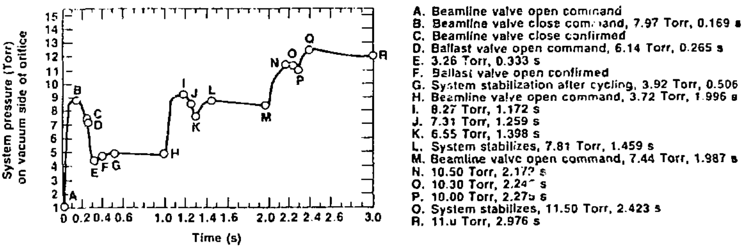

Fig. 11 Averaged results of system pressure response on vacuum side of 10.0-mm ø orifice. 80-psi valve actuator pressure. Multiple cycles.

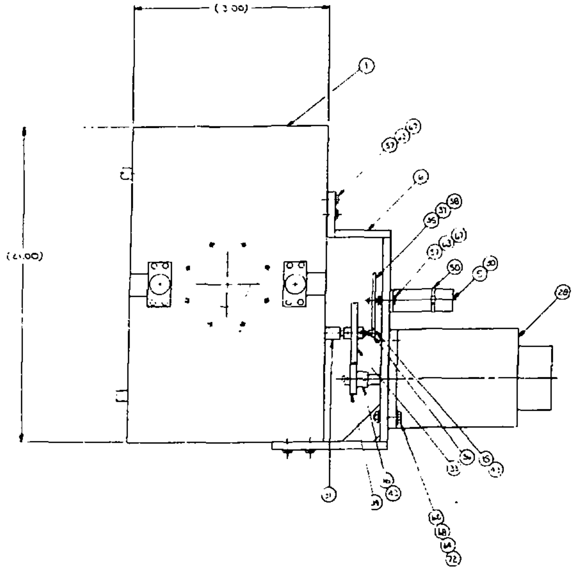

33	5310-21811	WASHER, LOCK 5/16 NOM S.STL	FF-W-92	68	1	P2053?X 40	GEAR, SPUR 20P, 40TEETH, 2.00 PD, ¼ BORE S STL	↓	34
44	5310 21883	WASHER LOCK ¼ NOM. S.STL	FF-W-92	67	1	P2053?X 80	GEAR SPUR, 20P, 80TEETH, 4.00 PD, ¼ BORE S STL	W.M. BERG INC	33
9	5310 21878	WASHER LOCK #10 NOM S.STL.	FF-W-92	66	2	121-DP	AIR CYLINDER DOUBLE ACTING ½ BORE 1.00 STROKE	BIMBA	32
				65	3	SOC123978	VACUUM FEEDTHRU MODEL #HB 250 [illegible] CBR	FERROFLUIDICS	31
28		WASHER, FLAT 3/8 NOM S STL		64	3	GECII-13P2	ENCODER PIN CONTACT	LITTON	30
56		WASHER, FLAT ¼ NOM S STL.		63	2	M063-FD09-E	MOTOR STEPPING DUAL AXIAL	SLO SYN	29
8		WASHER, FLAT #10 NOM S STL		62	1	M112 FD-301	MOTOR, STEPPING	SLO SYN	28
2	5305 47559	SCR SOC HD HEX 5/16-18UNC 2A × ⅝ LG. S STL	FF-S-86	61	1	2-284	O RING 3.975 I.D × .139 WALL BUNA N	PARKER	27
4	5305 20174	SCR HEX HD 5/16-18UNC 2A × 1¼ LG S STL	FF-S-85	60					26
24	5305-20173	SCR HEX HD 5/16-18UNC 2A × 1½ LG S STL	FF-S-85	59	1	85-11793	MODIFIED MICRO SWITCH		25
8	5305-20161	SCR HEX HD ¼-20UNC 2A × 1½ LG S STL	FF-S-85	58	2	85 11792	SMALL MICRO-SWITCH BRACKET		24
16	5305-20149	SCR HEX HD ¼-20UNC 2A × 1.00 LG S STL.	FF-S-85	57	1	85 11791	SPROCKET DRUM ASSY		23
22	5305-20148	SCR HEX HD ¼-20UNC-2A × ⅞ LG S STL	FF-S-85	56	1	85 11790	MICRO SWITCH BRACKET TAB 02		22
2	5305-20784	SCR FLAT HD 82°, ¼-20UNC 2A × ⅝ LG S STL	FF-S-92	55	1	85 11790	MICRO SWITCH BRACKET TAB 01		21
8	5305-47642	SCR SOC HD HEX #10-32UNF 2A × 1.00 LG S STL	FF S-86	54	2	85-11781	ROLLER BRACKET TAB 02		20
				53	1	85 11780	SPRING ROLLER BRACKET TAB 02		19
1	5935-68363	CONNECTOR MULTI PIN RD HERMETIC S STL	[illegible]	52	2	85 11789	AIR CYLINDER BRACKET		18
1	5935 68359	CONNECTOR MULTI PIN RD HERMETIC S STL	[illegible]	51	2	85 11788	AIR CYLINDER COUPLING		17
3	4730-14437	HOSE CLAMP 1⅛ Ø NOM. S STL.		50	1	85 11787	LARGE MOTOR COUPLING		16
3	BA2RV-A2	MICRO SWITCH	[illegible]	49	1	85 11786	FEEDTHRU COUPLING		15
8	S 2OO14	BEARING ANGULAR CONTACT, .3125 I.D × .6875 O.D S STL	BARDEN	48	1	85 11785	FOIL (KAPTON) TAB 02		14
4	PE21-3	SCR SHOULDER #10-32UNF 2A × .2495 Ø × .500 LG S STL	WM BERG INC	47	1	85 11785	FOIL (TITANIUM) TAB 01		13
4	PZ18-3	SCR SHOULDER #10-32UNF 2A × .1495 Ø × .188 LG S STL	↓	46	2	85 11784	SPRING ROLLER		12
4	SC6-28	SET SCREW SILVER TIP #4-40UNC 2A × 3/16 LG S STL.		45	1	85 11783	ROLLER		11
2	SC6-1	SET SCREW, SILVER TIP #2-56UNC 2A × ⅛ LG S STL.		44	2	85 11782	ROLLER MOTOR DRIVE		10
2	SC2-3D	SET SCREW #6-32UNC 2A × ⅛ LG S STL.		43	2	85 11781	ROLLER BRACKET TAB 01		9
2	CT19	SLEEVE COUPLING ⅛ TO 3/16 SHAFT Ø S STL		42	1	85 11780	SPRING ROLLER BRACKET TAB 01		8
2	CT3	SLEEVE COUPLING ⅛ SHAFT Ø S STL.		41	2	85 11779	SMALL MOTOR BRACKET		7
2	CG3-11	SPLIT HUB CLAMP ⅛ Ø SHAFT S STL		40	1	85 11778	LARGE MOTOR BRACKET		6
2	PE3-6	SHAFT EXTENSION .2498 BORE × .1872 Ø SHAFT S STL		39	3	85 11777	ENCODER BRACKET		5
3	CG3-7	SPLIT HUB CLAMP 3/16 Ø SHAFT S STL		38	1	85 11776	CLAMPING PLATE		4
2	PE3-7	SHAFT EXTENSION .1248 BORE × .1872 Ø SHAFT S STL		37	1	85 11775	SEALING PLATE		3
3	PA521 30	GEAR SPUR W/P 30TEETH .4687 PD, .1870 BORE S STL		36	1	85 11774	COVER		2
3	PA521 240	GEAR SPUR W/P 240TEETH 3.75 PD, .1870 BORE S STL		35	1	85 11773	FOIL MECH HOUSING		1

Fig. 12 Foil mechanism assembly drawing.

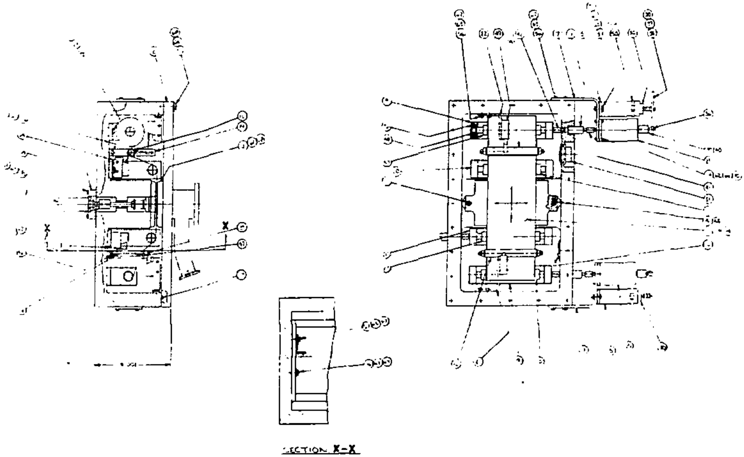

Fig. 13 Foil mechanism internal view assembly.

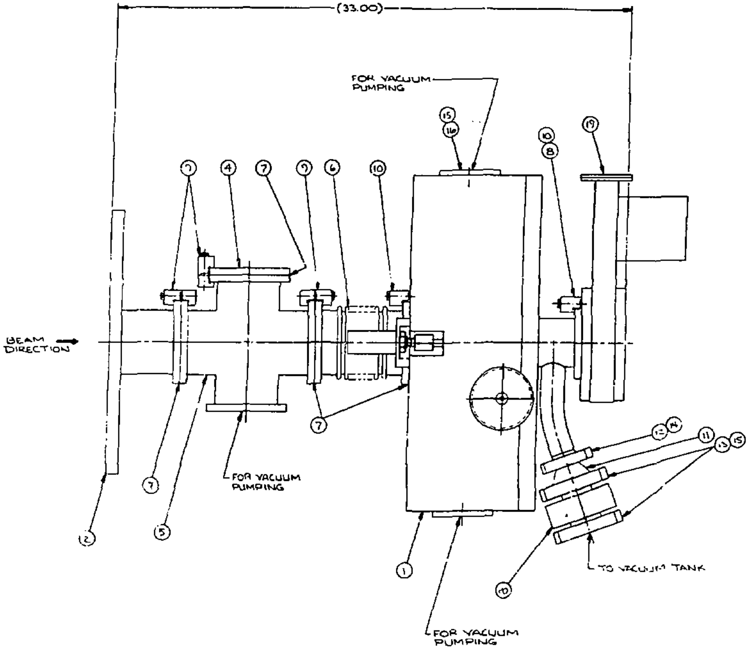

				21
1	VRL0266-SPECIAL	GATE VALVE 2	VRC	20
1	14040PEB0X	GATE VALVE, SERIES 14 SPECIAL	VAT	19
				18
				17
2	31-6906	CLAMP BULK HEAD [illegible] NW 50	MPS CORP	16
4	31-2506	CENTERING/SEAL ASSY NW50		15
1	31-2505	CENTERING/SEAL ASSY NW40		14
2	31-2906	CLAMP WING NUT + SCREW CLOSURE NW 50		13
1	31-2905	CLAMP WING NUT + SCREW CLOSURE NW40		12
	31-3716	REDUCER 150 KF NW40 TO 50 S.STL		11
16	76-1006	CLAMP SINGLE CLAW NW100/NW80		10
24	76-1106	CLAMP, DOUBLE CLAW NW100		9
1	76-0708	CENTERING/SEAL ASSY NW80		8
4	76-0710	CENTERING/SEAL ASSY NW100		7
1	76-3510	BELLOWS 150-MF FLANGES NW100 S.STL		6
1	76-1510	CROSS 150-MF FLANGES NW100 S.STL		5
1	76-0110	FLANGE, MF, BLANK NW100	MPS CORP	4
				3
1	85-111757	ADAPTOR SPOOL		2
1	85-111758	FOIL MECH ASSY		

Fig. 14 Vacuum/air interface assembly with foil mechanism assembly.

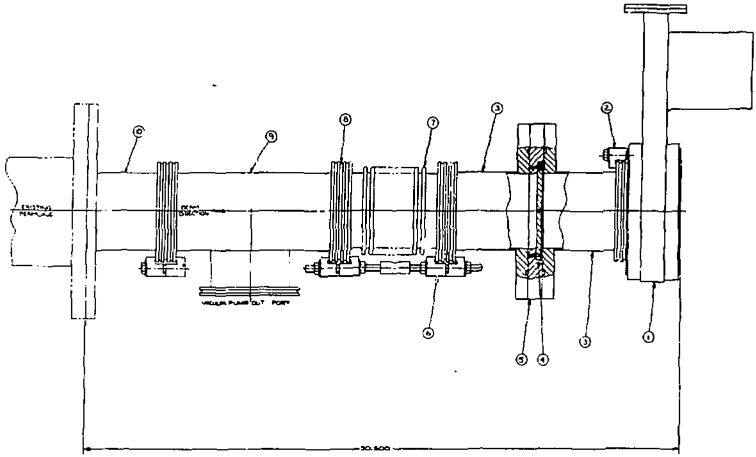

Fig. 15 Vacuum/air interface assembly with orifice assembly.

DISCLAIMER